An Attitude Control Design for the Cassini Spacecraft

Edward C. Wong, William G. Breckenridge
Jet Propulsion Laboratory
California Institute of Technology
Pasadena, California 91109

The Cassini planetary mission to Saturn and Titan requires accurate pointing and complex maneuvers of the spacecraft, which is comprised of a Saturn orbiter and Titan probe. An attitude control design is described to achieve the many capabilities of Cassini including thrust vector control, precision pointing and stability control for remote sciences, tracking of a probe released to the Titan atmosphere, and radar mapping of the Titan surface. Additional constraints for control design have been imposed by a high percentage of liquid propellant (60.% at launch) and lowly damped flexible spacecraft appendages. Computer simulation results of attitude determination, pointing and maneuver controls are provided to demonstrate the design capability.

1. Introduction

1.1 Mission and Science Objectives

The Cassini spacecraft to Saturn and Titan is scheduled for launch in 1997, and will arrive at Saturn in 2004. It will orbit the inner solar system to pick up Venus and Earth gravity assists, followed by Jupiter flyby and Saturn orbit insertion. Probe entry to the atmosphere of Titan will occur about four months after Saturn arrival. Unlike both Voyager 1 and 2 which flew by Saturn but did not go into orbit, Cassini's mission will include four years of Saturn/Titan orbiting tours. Cassini science objectives include investigation of Saturn's atmospheric composition, winds and temperature, configuration and dynamics of the magnetosphere, structure and composition of the rings, characterization of the icy satellites, and Titan's atmospheric constituent abundance. The radar mapper will perform surface imaging and altimetry at each Titan flyby.

Cassini was originally one of the two spacecraft of Mariner Mark 11 series intended for multi-mission purpose: the CRAF (Comet Rendezvous and Asteroid Flyby) and Cassini. The CRAF mission was to follow a comet and conduct scientific investigations for 120 clays and later flyby an asteroid. Budget constraint demanded the deletion of CRAF and its associated mission objectives, payloads, and capabilities. The Cassini spacecraft as originally conceived was also descoped. Both the high and low precision scan platforms and their structural booms were deleted to reduce the effects of structural flexibility. This means additional control of spacecraft basebody is necessary to achieve high gain antenna earth pointing, star tracking, and remote science pointing. A turn table for fields and particles experiment was deleted. Therefore, additional rolling of spacecraft is necessary for fields and particles science that would otherwise be done by a turn table. The result is one Cassini spacecraft with descoped capabilities, and yet will deliver a good portion of its originally intended mission objectives.

1.2 Spacecraft Configuration and Modeling

Cassini is a flexible spacecraft containing four structural booms and three propellant tanks. The deployed Cassini spacecraft with the Huygens Titan probe is shown in Fig. 1. The four attached booms are a magnetometer boom and three radio and plasma wave. science booms. The middle structure of the spacecraft is the propulsion module consisting of two elliptical tanks for bipropellant. At the bottom of the propulsion module is the lower equipment module, which supports three radio-isotope thermoelectric generators, four reaction wheels, a probe relay antenna, and two articulable (two axis) main engines for large trajectory corrections and Saturn orbit insertion.

At launch, the spacecraft total mass is approximately 5570 Kg and inertia is [8970, 9230, 3830] Kg-m^2. Towards the end of the Saturn tour phase with the probe released, the mass will be reduced to 2700 Kg and inertia to [6510, 5290, 3478] Kg-m^2. The spacecraft is modeled by a flexible core structure but with rigid appendages (propellant masses, main engine gimbals, and reaction wheels). The equations describing the flexible core body are generated from Nastran model data. Due to the absence of articulable rigid element at the end of the flexible booms, no modal reduction process of any significance is necessary. The magnetometer boom has a fundamental frequency at 0.65 Hz and damping between 0.2 to 1.0 %. The three radio and plasma wave antennas are much lower in mass and inertia, and have a frequency of 0.13 Hz or higher and a damping of 0.2 %.

At the beginning of the mission, the spacecraft propellant is heavier than the spacecraft dry mass. The spacecraft has two bipropellant tanks and one monopropellant tank. The bipropellants, burned by the main engine and has total mass of 3000 Kg, are monomethyl hydrazine (MMH) and nitrogen tetroxide (NTO). The tanks are cylindrical with hemispheric end domes, and "stacked" along the spacecraft Z axis. The monopropellant is hydrazine and burned by the attitude control thrusters. Its mass is 132 Kg. The tank is spherical and off the Z axis. The bipropellant tanks contain an 8-vane propellant management device.

The spacecraft is in "low-g" environment when the spacecraft is limit cycling or during thruster maneuvers. When the spacecraft is under high acceleration delivered by the main engine force of 440 N, it is in the "high-g" environment. Both high and low-g propellant slosh are modeled as pendulums with torsional spring and defined by model data at different tank fill levels. In the case of low-g, the propellant is dominated by surface tension effects, and is attached mainly to the core of the propellant management device and the tank wall. When acceleration is created by firing the attitude control thrusters for delta-V burns or turns, part of the propellant goes to the "bottom" of the tank, but surface tension is still relatively dominant. Damping is expected to be over 10940. However, not all the propellant mass is sloshing. Only 25-68 % of the total liquid participates in the sloshing motion, depending on the propellant fill fraction. Slosh frequency in low-g is nominally between 0.003 and 0.006 Hz [5].

The high-g force basically dominates the surface tension force in affecting the propellant motion . When the main engine fires, the propellant would be leveled to the "bottom" of the tank. Once the main engine firing stops, the propellant would reorient itself back to the zero-g orientation in less than 5 minutes. Damping is expected to be between 10-30 %, and only 25-4570 of the total liquid participates in the sloshing motion, depending on the fill fraction. Slosh frequencies at high-g is at around 0.06 Hz and 0.14112.

Propellant slosh effect on the spacecraft is proportional to the propellant mass which is a decreasing function of mission time. On the other hand, the propellant mass contributing to slosh increases with decreasing fill fraction. The maximum net propellant sloshing effect is at near 50 % of propellant fill

level. However, most of the remote science pointing is done in the tour phase when the spacecraft is orbiting around Saturn. At that stage, a large portion of propellant has been depleted for Saturn orbit insertion, and the remaining propellant of 20-30 % fill fraction would be modeled for disturbance in flyby scenarios and remote science pointing.

2. Attitude Control Functions

The primary Cassini attitude control functions are attitude determination, attitude command generation, attitude turns and pointing control, spacecraft burn maneuvers, constraints avoidance, fault protection, command processing, telemetry generation and data handling. This paper covers the areas of attitude determination, attitude command generation and attitude control.

The attitude control software is contained in the flight computer which communicates with a separate computer for command and data handling. The onboard control software runs at a computational cycle of 8 times per sec. Attitude control is supported by its peripheral sensors and actuators. They are the digital sun sensors and star tracker for celestial reference, accelerometers for spacecraft velocity change or delta-V, gyros for inertial attitude motion, reaction wheels and engine gimbal actuators for control actuation, and the propulsion valve electronics for valves, attitude control thrusters, main engines and heaters control,

The attitude control functional block diagram is shown in Fig 2. After the spacecraft attitude is initialized using the sun and star, the spacecraft will maintain knowledge of its attitude with respect to the celestial coordinate system at all times based on the star identification and attitude estimation outputs. The celestial coordinate system is called the "J2000" which is an inertial frame defined by the Earth Mean Equator and Equinox at the year 2000 epoch. Ground commands are uplinked to the spacecraft onboard software, and the spacecraft will generate the corresponding turn command profile. The controller will hold to a commanded attitude such as pointing to the Earth, or it will faithfully follow a commanded turn profile which can vary in both turn axis and turn rate in order to accomplish functions such as surface mapping, single axis roll turn for fields and particles science, and probe tracking by the high gain antenna. Turn and attitude hold are usually done by the reaction control subsystem thrusters, except for precision pointing and slewing for remote sciences which are done by reaction wheels. Spacecraft delta-V is imparted through either a main engine for large burn maneuvers or thruster pulsing for the smaller bums, which are done only in one body-fixed direction (-Z). Constraint violations of turn commands are checked and avoidance path is generated, if necessary, by onboard software prior to command execution by the attitude controller.

2.1 Challenges to Cassini Control Design

The Cassini attitude control design has to satisfy stringent pointing and control requirements imposed by the mission. Extraordinary effort has been spent to design capable and reliable onboard control system software. Such a design should be capable of high adaptability and modularity for future changes and updates, such as the ability to regroup or descope capabilities, if necessary, with relative ease and simplicity.

The spacecraft is required to point the high gain antenna to Earth to within 2 mrad accuracy (3 σ) and to roll about the antenna boresight (-Z) axis at 0.26 deg/sec for fields and particles measurement while

maintaining Earth downlink. For remote sciences (imaging, infrared spectrometry, etc), the spacecraft is required to achieve pointing accuracy of 2 mrad (3σ) and maintain stability of spacecraft motion over a variety of time windows at the completion of a slew allowing 20 sec of settling time. Typical stability requirements at staring mode are 4 μrad (2σ) over 0.5 sec time window and 160 μrad (2σ) over 100 sec time window in root-mean-square sense.

There are extraordinary constraints imposed on the controller design due to propellant slosh and structural effects. At launch, 60 % of the spacecraft is liquid propellant. The possible excitation of the large amount of liquid propellant indicates a big challenge to both the control design for stable pointing of the spacecraft, and the need of a fairly accurate modeling of the propellant characteristics, such as frequency and damping of the slosh modes. Since propellant slosh is relatively difficult to model, the approach taken for Cassini's control evaluation is to develop a mechanical-analog model that conservatively bounds the disturbance effects due to propellant motion such that the worst case effects can be captured in the control design evaluation [1][5]. The spacecraft control system should also be designed with sufficient margin from unstable interactions with the flexible appendage of science instruments, such as the magnetometer boom and three radio and plasma wave science booms. The spacecraft is also required to maintain a slow turn within a 1 1/2 hours of main engine burn during Saturn orbit insertion.

Much emphasis has been given towards driving the control and software design towards autonomy, modularity and fault tolerance to accommodate the 12.-year mission life, long round-trip light time, and reduced ground mission support and cost, as well as the flexibility to prepare for possible system design changes.

2.2 Control Architecture

Fig. 3 shows the Cassini spacecraft control architecture which takes the approach of an "object-oriented" design. The architecture contains many control functions or combination of algorithms called objects. The software modules such as the attitude commander, attitude controller, and the Sun Sensor manager (software-to-hardware interface program) are each an object. The architecture contains three levels of object hierarchy: the top level commander determines the control modes and generates profiled commands, the mid-level controller and estimator executes the commands, and the low-level hardware managers provide the interface with hardware as needed. The long arrows show the procedural calls or events, and the short ones indicate the direction of data flow. The. high level objects (commanders) and the low level objects (hardware managers) are, to a great extent, decoupled. Such is an object-oriented design feature which requires that each object should be told by its client (object which invokes the procedural call) only what it needs to know to do its job. For example, the 10W-1CVC1 hardware manager objects do not need to know the current attitude control mode to perform their functions.

The mode commander represents the highest level object in the control software architecture. It indicates mode switching and coordinates the commanders and controllers below it for more specific tasks. The attitude commander generates position, rate and acceleration command profiles for pointing. The command profile is sent to the attitude controller which computes attitude and rate errors based on the attitude estimator's output for generation of control torque to the hardware device. The attitude controller then follows the command profile in an attempt to minimize the target quaternion error at all times, regardless of whether the maneuver is done by reaction wheels or thrusters. The attitude controller also controls translation (delta-V) maneuvers.

The attitude estimator is the central repository of all the angles and rates derived from either measured or processed attitude control sensor data. Consequently, all the attitude data needed by other control functions will be requested from the attitude estimator. The attitude estimator is operative in all attitude control modes, and is capable of working with complete or partial sensor data such as a temporary loss of star or gyro data.

The low level objects in the architecture are the hardware managers. They do very specific interface functions with the hardware devices, such as, send torque commands to the actuators or read sensor data. The also contain misalignment parameters to be calibrated and compensated onboard (e.g. gyro and accelerometer drift). Because of their proximity to hardware raw data, they also monitor data consistency or reasonableness and signal warnings to the fault protection software if a fault is detected.

The Cassini control architecture also contains a constraint checking and avoidance feature not described in detail in this paper. Profile commands generated by the attitude commander will be continuously monitored by such constraint monitor. In theory, the commander generated profile should never violate a constraint region if the ground command sequence is generated properly. However, in the event that an attitude profile brings an instrument boresight into a constraint region (such as the sun), the Cassini software would do its best to generate an alternative commanded path of acceptable rate or acceleration before being passed along to the attitude controller for further spacecraft turns. The spacecraft will follow the alternate path until it eventually catches up with the originally intended command path.

2.3 Control Design Overview

The attitude control approach for the Cassini mission is primarily determined by whether it is gyro or non-gyro based. The spacecraft will spend most of its mission time in the non-gyro based attitude control where attitude knowledge is provided by the attitude estimator and spacecraft limit cycle control for high gain antenna Earth pointing is performed by thrusters. Here, the attitude estimator propagates the primary states of 3-axis attitude errors and rate at 125 msec cycles by a rigid body dynamic model. Stars are usually available and measured by the star tracker. The propagated attitude will be corrected periodically (every 5 see) by this absolute inertial reference. The controller is bang-bang type, with linear switching line and adjustable deadband size. Since attitude limit cycle motion is generally quite slow with rates mostly below 50 ~rad/see, a low-rate controller submode is used. It is designed to optimize the thruster pulsing duration and "walk" the attitude deadband to alleviate noise-induced multiple pulsing in order to preserve the consumable thruster valve operation cycles.

When the spacecraft is required to turn, to do bum maneuvers, or to do precision pointing, attitude control will be required to go to gyro-based. Much better attitude knowledge can be determined by the combined star and gyro data, and attitude control will be performed by reaction wheels, attitude thrusters or a combination of main engine gimbals and thrusters. Here, the attitude estimator goes to six primary states of 3-axis attitude errors and 3 gyro bias, and nine secondary states of gyro scale factors and misalignments. The drift-compensated gyro output will be integrated by a gyro-based quaternion integrator to give the propagated attitude and with periodic star updates every 5 sec. Gyro drift rate is estimated and corrected onboard. All the gyro-based controllers are sampled at 125 msec. The reaction wheel controller design consists of a 3-axis proportional-integral-differential controller with 0.03 Hz bandwidth. The controller also contains a fourth-order filter for limiting noise in the rate feedback. Design has been

optimized to suppress low-g slosh modes, and yet to leave sufficient stability margin from the possible interaction with the radio and plasma wave science booms.

Spacecraft stabilization after probe ejection and Centaur tip-off, fast turns, and surface or limb tracking during flyby of Saturn moons are performed using attitude thrusters. Again, a bang-bang linear switching line controller with adjustable deadband size is used. A second-order notch filter is implemented in the controller to prevent disturbance induced oscillation of the magnetometer boom. The requirement by this notch filter of a prior knowledge of magnetometer boom frequency to within 20 % is considered within capability.

Equally important is the design of stability margin of the thrust vector controller for main engine burn maneuvers. Here, a higher controller bandwidth of 0.2 Hz is necessary to stabilize the spacecraft and keep the rate down during the burn transients using the 440 N engine. 'I'he propellant high-g slosh mode and magnetometer fundamental boom mode are possible source of interactions that can destabilize the thrust vector controller.

In the following sections, attitude determination, pointing command generation, attitude control design and their selected simulated performance are described in more detail.

3. Attitude Determination

3.1 Star Identification

The star identification (Star ID) algorithm has three primary functions. It initializes spacecraft attitude, identifies and continuously tracks stars, and re-acquire the star set if star tracking is interrupted. Initial acquisition is done after launch and subsequent acquisition is necessary when attitude is lost upon fault recovery. Once multiple stars are acquired within the 15 deg field-of-view (FOV), star ID will transition to track mode. In track mode, each star's location relative to the tracker 1024 x 1024 charge couple device (CCD) coordinates are provided to give the 3-axis attitude. The Star ID controls star tracker window positions and sizes, star image integration times, and if necessary the summation of pixels for coarse star acquisition at higher spacecraft rates. It computes star centroids and their intensities from pixel data. It also has access to the onboard star catalog, which contains approximately 4000 stars, and selects and uses only the stars within the catalog.

As a sensor processing function, Star ID has a large amount of data to be processed, such as star catalog and pixel data. It takes more time to execute Star ID than any other algorithms. This is because the tracker does not have the desired measurement ready immediately upon sampling by the flight computer, and there are long delays between functions, such as between the completion of pixel data collection and the completion of pixel data processing in the computer to determine centroid positions.

Attitude Initialization

The attitude initialization function of Star ID is usually initiated when the attitude uncertainty of the tracker is too large to use the priori attitude estimates to position windows about the catalog stars. It nominally can tolerate an attitude uncertainty up to 2 deg per axis. Attitude initialization extracts the likely star candidates, such as bright spots, from pixel data. It then focuses on more accurate spot position measurements. The star search region is greatly reduced by having a measurement of the direction to the

sun, and thus the sun-to-star angles, to about one degree accuracy. It then extracts stars from the onboard star catalog, and exercises an algorithm to match measurements to stars. The sun-to-star and star-to-star angles are used in the matching.

For attitude initialization, pairwise computations between stars are made. Such computation has enormous numerical complexity. For example, it takes about fifty thousand multiplies to compute the pair separations for 100 stars. As the number of stars (n) grows, the pairwise check increases on the order of n2. The expected nominal time taken in an attitude initialization is between 10 to 20 min of computational time. Using sun-to-star angle and magnitude to limit the number of stars that might match a measured "spot" reduces the complexity of the identification process.

Star Tracking

Unlike attitude initialization that determines which stars are in the tracker FOV, star tracking function determines where to place the windows on the stars that are already known to be within the FOV. Star tracking performs a pixel search routine to locate bright spots and to decide whereto place the track window. There will be continuous star hand-offs when the spacecraft is in motion which changes the sky coverage. To be qualified for the "best" candidate of the next star to be selected, the star must have the most angular separation from any other stars in the current star set (minimum 5 degrees). Proper star tracking also requires a minimum number of two stars in the star set, but up to 5 stars are usually being tracked during normal operations.

The software computes the centroid positions. Centroiding includes stray light and background subtraction, bright pixel compensation, and limited image shape validation to reject bright objects or pixels. The algorithm also calculates the distortion corrections based on the star color stored in the catalog, and predicts the star positions in focal plane coordinates. The final check is to verify or identify the stars based on the star-to-star and measurement-to-measurement separations. If there is difference in measurement and catalog values, this will add to the level of uncertainty, and will be a criterion to reject a measurement. The star positions are compensated for velocity aberration which are offsets due to speed of spacecraft perpendicular to the line of sight of the star tracker. The star positions are then sent to the attitude estimator, along with the measurement uncertainties.

Any star identification failure during this tracking process will cause the estimator uncertainty to increase and Star ID to search larger areas for stars. Continued failure will trigger a transition to star re-acquisition.

Star Re-A cquisition

The star acquisition function is an intermediate stage between the. initialization and track functions. It serves to acquire stars subsequent to star initialization, or to re-acquire stars when stars are temporarily drifting off the track window due to larger than expected attitude motions during star tracking. It commands *one* large track window at a time. The pixel data is scanned, as in the initialization mode, but the star set used for matching is constrained to the expected stars being tracked.

Star ID algorithm goes to large windows to locate "isolated" stars to reinitialize attitude. The regular track function uses window up to 40 by 40 pixels (1/4 mrad per pixel). Taking the approach of summing up a 4x4 pixel to be a "super-pixel" for re-acquisition, this allows a track window to cover a 40 mrad square FOV. When the attitude uncertainty becomes larger than about 5 mrad but below 40 mrad in

one axis, Star ID rescans the entire track window for star data. If star is found, the estimate is used for the window placement on the next track frame. If the stars on the track frame are found and re-identified, the Star ID transitions to the track mode. Otherwise another reacquisition attempt is made. Continued failure will cause a transition to attitude initialization.

3.2 Attitude Estimation

The attitude estimator provides the estimate of spacecraft attitude and rate estimates from star and gyro measurements. Its propagation and estimation methods vary in different phases of the Cassini mission due to sensor data availability. At launch when only gyro data is available, the attitude is propagated using gyro measurements, and the estimator output is used for controlling spacecraft rate from launch vehicle tip off and later searching for the sun. Once sun data is available in addition to the gyros, they are processed to compute attitude estimate corrections, needed to compensate for gyro drift and spacecraft motion with respect to the sun. While the spacecraft is controlled to keep the sun near the center of the sun sensor FOV with rate controlled about the sunline, the Star ID processes the star data to identify the stars in the star tracker FOV and computes the spacecraft attitude with respect to the J2000 coordinate frame. Once star reference is established, the spacecraft will operate and remain in celestial coordinate frame for most of the Cassini mission, The J2000 attitude knowledge can be lost is through an anomaly, in which case a sun search may be needed tore-initialize the attitude.

During the cruise period, gyros are turned off to preserve their life. time, and the spacecraft attitude is propagated using a rigid body dynamic model carried in the estimator. The applied thruster or reaction wheel torque impulse is used to drive the dynamic model for attitude propagation. The use of a dynamic model results in degraded accuracy and robustness and, therefore, is used for low accuracy applications such as cruise control and other low accuracy science.

For precision pointing and attitude stabilization, gyros are turned on in addition to the star tracker, allowing the spacecraft to have both celestial and inertial references. This sensor data combination produces 'higher accuracy in attitude and rate estimates used for high accuracy remote science, antenna pointing, and delta-V maneuvers. In this mode of operation, gyro data is used to propagate the attitude quaternion while star data from the star tracker is used to introduce corrections in the spacecraft attitude estimate and the gyro parameters such as biases, scale factor, and misalignments.

Star Identification Interface

Once the attitude estimator has a celestial reference, it receives data from Star ID in the form of a Star ID table. This table is generated by Star ID asynchronously once an image has been exposed and read from the tracker and the resulting star measurements have been positively identified, The data in the table is associated with only one exposure of the tracker, and because of the limitation of the tracker hardware, it can not contain more than 5 identified star measurements. Star ID computes the extrapolated tracker attitude quaternion, the time associated with the saved attitude and attitude rate estimate used in the extrapolation, and a star set change index which indicates when a change in the set of identified stars has occurred. The rest of the table consists of the measured value, measured uncertainty and predicted value of two normalized focal plane coordinates of each identified star. The standard deviations of the measured uncertainty represent a measure of the quality of the observations. The predicted values are based on the attitude estimate at measured time mapping star vectors to the focal plane. After filling up the Star ID table,

Star ID waits for the estimator to complete the pre-filter data processing before starting a new star identification cycle that would lead to new content in the Star ID Table.

Attitude State Propagation

The attitude-estimator computes in every software cycle an estimate of the change in spacecraft attitude. If the estimator is on gyros and sun sensor, this estimate is compensated for bias, scale factor, and misalignment errors. If the estimator is on star tracker only, the attitude propagation is generated using a rigid body dynamic model of the spacecraft. The spacecraft angular acceleration is a function of the torque applied by wheels or thrusters about spacecraft center-of-mass, and estimates of disturbances such as gyroscopic torque. The angular acceleration computed will have fairly large errors up to 10% due to errors in the knowledge of spacecraft inertia properties, thruster impulse prediction, reaction wheel scale factor, etc,

With gyro data available, the spacecraft attitude propagation is computed by a second-order quaternion integrator, processing the drift-compensated gyro pulses as was done on Galileo [4]. On previous planetary spacecraft, the gyro was calibrated by ground processing. Calibration gyros onboard requires only a larger number of elements in the estimator state, but has the benefit of significant cost savings in ground processing and telemetry.

covariance Propagation and Attitude Update

The chosen attitude estimator architecture tries to achieve a balance between high attitude estimation performance and low computational complexity. It consists of a pre-filter that statistically combines all the star measurements that take place within the time interval that comprises the state propagation time interval (5 see) into a single three axis pseudo measurement with its corresponding uncertainty that is fed to the Kalman filter. The Kalman filter then propagates the covariance across the same time interval and incorporates the pre-filter pseudo measurement to come up with a correction to the state estimate. The corrections are not applied until the start of the next time interval. This way, the pre-filter would not need to be informed of the filter state correction and perform additional computations to accommodate them. By delaying the application of the corrections to the beginning of the next time interval, not only the design of the pre-filter, and its interface, is simplified but also the behavior of the whole estimator becomes more predictable.

The Kalman filter formulation requires onboard propagation of the covariance matrix. The covariance also serves as a measure of attitude and rate estimate quality, and can be used by star ID to set the correct window size before its star acquisition. For this reason, we want to propagate the covariance matrix at regular intervals, even in the absence of measurements. The estimation of the gyro scale factor and misalignment parameters can be turned on and off depending if a planned calibration maneuver is underway. Star ID identified star vectors are used to compute corrections to the propagated attitude quaternion estimate. The time intervals at which these corrections are computed is a flight adjustable parameters nominally set at 5 seconds intervals.

Although most star tracker measurement noise can be assumed Gaussian with zero mean, some error sources, such as tracker optical distortions behave like biases that depend on the star geometry. A star set change results in change of biases which could introduce large step change in the attitude estimate. To cope with star set change which is inevitable when the spacecraft is turning, the estimator would use the new star set information gradually. This can be accomplished by increasing the measurement noise

variance upon the occurrence of a star set change, and subsequently decrease the noise exponentially within the period when no such change occurs.

Fig. 4 shows the simulated performance of the attitude estimator in the convergence of estimates in attitude and gyro bias using a nominal star sets. The envelope is the 3σ attitude error computed by the covariance matrix. A star set change occurs at the beginning of the estimation process in order to trigger the estimator's optical distortion compensation. The spacecraft axis (X) along the star tracker boresight is the worst axis in knowledge accuracy. Even so, the attitude estimate error about that axis stays below 0.5 mrad most of the time. The gyro bias estimate converges in around 20 min.

4. Command for Attitude Pointing

Cassini builds on features implemented on the Galileo spacecraft such as the ability to control pointing with respect to inertially defined moving targets. The targets were modeled on Galileo as a spacecraft centered position vector with constant linear velocity. On Cassini, target vectors are propagated as conies or polynomials. This enables the commander to benefit from fixing its reference coordinate frame with respect to the moving target. In this section, we first describe how vectors are propagated, and then the method of how turn commands are generated.

4.1 Inertial Vector Propagation

On Cassini, the information on the location of inertial objects in space around the spacecraft are propagated by the inertial vector propagator. These are target objects to be pointed by the antenna or science instruments. In the inertial vector propagator, celestial target positions are connected in a tree-structure. Spacecraft-to-target is the sum of vectors along the spacecraft-to-target path. To determined the location of a target from the spacecraft, it may be necessary to follow a path through two or more component vectors and the polarities of addition which results in the desired spacecraft-to-target vector. During the Saturn tour, the Earth is usually found by following a vector path through three entries: spacecraft to Saturn, Saturn to sun, and sun to Earth. During a close flyby of Titan, the path would contain one more entry, spacecraft to Titan, and Titan to Saturn. Once the path to a target is known the vectors along the path are added to produce the target location. The resulting structure must always be a tree.

At the velocities traveled by the spacecraft, the speed of light actually makes a significant contribution to the pointing error. The error, if uncorrected, would exceed the fitting requirement for inertial vectors. The speed of light correction is done by onboard algorithms whenever a complete target path is calculated, with the correct sign for correction determined by a ground command.

Vectors Tables

The primary data base for inertial vector propagation is an inertial vector table which describes the motion of objects that the spacecraft point to, such as Earth, sun, Saturn, Titan, etc. Each vector in the table is an object's position and rate relative from another. An example of a table entry is the vector from sun to Earth. In cruise, an entry is from sun to spacecraft. During the Saturn tour, an entry can be the vector from Saturn to the spacecraft, or from sun to Saturn. The inertial vector table is designed to carry up to 50 entries. Any object named in the table is required to appear only once as the head of a vector. (For a vector from point A to point B on the tree, A is referenced to as the base and B as the head), Such head name is unique, thereby entries can tie to names, not location in the table. Furthermore, every identified

base is required to exist somewhere in the table as a head except for the sun. An entry can be moved from one base to another without violating this rule, such as the base of the vector to the spacecraft can be moved from Saturn to Titan. However, when entries are deleted, all entries left without an attached base must also be deleted.

A target table is also created to reduce the overhead of path calculation. When a new path is requested, it is first determined and a new entry is created in the target vector table which records the computed path so that the path does not need to be re-computed upon future requests. The creation and maintenance of this table is completely autonomous. The target table is empty at initialization. Most paths will typically remain active for long duration. The table entries not used for a specified period of time are deleted automatically. To protect from inadvertent deletion, the active component vectors are marked and are thus protected.

In order to relate pointing the parts of the spacecraft to the targets specified by the inertial vectors, a third table storing all the body vectors is created. Each entry of this body vector table is a fixed unit vector in body coordinates such as the high gain antenna, the narrow angle camera boresight, or a body principal axis. As will be described in a later section, the contents of this table enable the attitude commander to align the body vectors to the propagated inertial target vectors.

Background Propagation of Inertial Vectors

Once a target request is sent to the inertial vector propagator, the spacecraft-to-target vector is computed. Propagation of such vector is best done in the background. On Cassini, conies or polynomials are used to propagate inertial vector tree branches in the background. Conies are used for long duration propagation and polynomials are used for non-conic path for better accuracy. Conic background propagation uses the relative motion which satisfies the differential equation in the inertial position vector of the orbiting body relative to the dominant central body. The differential coefficient is a gravitational parameter, which is the product of the universal gravitational constant and the sum of the masses of the orbiting and the central bodies. When no other bodies are present, the motion follows a true conic of a two-body system. But the perturbing influences of other bodies around forces the motion to deviate from a true conic propagation. However, the true motion may still be approximated very well by a series of patched conies where each conic is chosen such that across one segment the deviations of the conic approximation from the true path are kept small.

The essence of a conic propagation is the evaluation of the position and velocity of one body relative to the other at some time in the future or past given the position and velocity of such body at another time. Equation for such evaluation (Kepler's equation) must be solved iteratively. The number of iterations required to converge is very strongly dependent on the required vector propagation accuracy. There are tradeoffs between accuracy and execution speed which is flight computer dependent. In the case of Cassini, it is required to propagate vectors with directional accuracy of 40 μrad for science pointing. Such accuracy requirement can be met.

When the conic approximation fails to keep the errors small for fitting the relative position vectors over a reasonable segment length, polynomial fits become the logical choice. Processes with perhaps the most attractive fitting characteristics are the Chebyshev polynomials. Chebyshev polynomials can be evaluated recursively and allows fitting a function of ephemeris with appropriate coefficients. Cassini's polynomial can be up to eleventh order. With such polynomial fitting the Titan-to-spacecraft vector at

closest Titan approach, a coverage of 2 hours duration is possible while meeting the directional accuracy requirement.

4.2 Attitude Command Generation

The attitude commander in the onboard software is responsible for generating attitude command profiles to point the spacecraft to any desired inertial attitude required for science or communication. Specifically, it generates turn profiles to bring the spacecraft from its last commanded attitude and rate state to another possibly time varying target attitude and rate state. A turn profile is generated based on commanded attitude, rate, and acceleration specified by the ground, and is required to be continuous in attitude and rates.

A command to re-orient the attitude is generated by applying a specified attitude offset to a reference attitude or "base attitude". An offset can be an absolute offset with respect to the original base attitude, or it can be an offset relative to the last commanded attitude. Once a base attitude is defined, the command profiling can proceed relative to this base attitude when given the angular offset, turn rate and turn acceleration.

Base A ttitude Generation

Commanding the attitude for inertial pointing can be described by first defining the base attitude, It would become clear why both target vectors and body vectors are defined in the form of tables as described in the previous section. The base attitude is established when two constraints are satisfied: The first or primary constraint is to align a body vector of interest, such as the high gain antenna or instrument line-of-sight, with an inertial vector of interest. The second or secondary constraint is to align a specified spacecraft fixed vector as closely as feasible to a specified inertial vector while maintaining the primary objective. Hence, if it is desired to point the camera to Titan, then the camera vector is selected from the body vector table and Titan from the target vector table. When these two vectors are aligned, the primary objective is satisfied, and likewise for the other degree off] eedom. The result is that the four vectors are coplanar. The attitude frame that satisfies these two constraint conditions is called the base attitude.

The main advantage of defining a base attitude this way is that the spacecraft attitude changes automatically when the targets move and hence target motion is automatically compensated. Furthermore, with the effect of target motion removed, it becomes simpler to do target relative pointing such as pointing to another feature relative to the target. However, as the computation to generate the base attitude is relatively extensive, it will be run at 1 second intervals to ease the computational load. In the mean time, the computed quaternion and rate are propagated, assuming, constant base acceleration, at every software cycle until the next instant of base attitude computation 1 second later, at which time an update of base attitude will take place.

Offset pointing

Once the target is fixed in view, a nominal pointing process is to stare at the target for a period of time for collecting images or move the instrument FOV across the target to capture more target information. On Cassini, moving the instrument FOV can be accomplished with offset commands. Offset commands define a rotation with respect to the base attitude. Since the base attitude is also defined as a rotation with respect to the inertial frame, the resulting attitude command defined by the offset is just the

product of these two rotations. All offset pointing are executed from the last commanded attitude and rate to the target attitude and rate established by the commands.

Attitude offsets are specified in terms of an euler axis and the magnitude of rotation angle about such axis. Offsets can be absolute or relative. The absolute offsets are relative to the base attitude. They are not cumulative. The resulted attitude rotation is always an offset from the base attitude. The offset euler axis is fixed in the base attitude. The other type of offset pointing is the relative or delta offsets. These offsets are always relative to the current target attitude. Unlike the absolute offsets, the relative offsets are cumulative. The cumulative offset is simply the combination of previously commanded offset turns. In this way, the target attitude is achieved by applying a cumulative attitude offset rotations to the base attitude. Absolute offsets are applied to the base attitude and the relative offsets are applied to the last target attitude.

Whenever there is a change in base attitude, a turn to the new target requires rate and position matching. In a rate matching phase, the rate error between the last commanded rate and the new target rate is removed. This introduces additional position offset which, along with the commanded offset, must also be removed during a position matching phase. In doing so, the actual destination will be reached but not in the manner in which it was prescribed since the rotation axis during the position matching segment is also dependent on the position offset introduced by rate matching. Therefore it is necessary to command an absolute offset following a change in base attitude.

Profiling sets peak rate and acceleration values in body coordinates to be used in offset turns. The values define an ellipsoid in the rate and acceleration space. The scalar rate and acceleration values to use are the points where the turn axis penetrates the rate and the acceleration ellipsoids. These angular rate and acceleration values determine the maximum allowable spacecraft motion relative to the base attitude.

5. Attitude Maneuver and Pointing

5.1 Attitude Control by Thrusters

Cassini uses reaction control thrusters to maintain 3-axis attitude control of the spacecraft for large or fast angular maneuvers (up to 0.75 "/see), sun search, rate detumble control such as after probe release and Centaur separation. The control thrusters also keeps the spacecraft within a limit cycle during the cruise phase. The propulsion module for attitude control is a blowdown system. The thrust level ranges from 1.1 N at the beginning of mission and 0.67 N at the end of mission with at least one re-pressurization in between. The spacecraft is on thruster control while momentum in the reaction wheels are unloaded about once or twice per week. Wheel momentum unloading is sequenced from the ground and is done in thruster control mode. A command is sent to change the wheel rate and the thrusters will hold the spacecraft within the control deadband until rate change in the wheels is completed.

Probe release into the Titan atmosphere is performed after a command is sent to switch attitude control into a "disabled mode". This is to avoid damaging the probe with combustion products from thruster firing during its departure from the spacecraft. The disabled mode will automatically time out after a few seconds, and the spacecraft will then execute a detumble maneuver. The detumble mode begins with an instrument boresight protection maneuver in which the spacecraft will slew about its Z axis (least inertia) at the maximum control torque such that the boresight of the remote science instruments (along the +Y axis) will not stay stationary in inertial space for too long. After probe release, the spacecraft will be

commanded to point the high gain antenna to the probe for data relay at a slow motion of 5 deg/hour but with a narrow deadband of +/- 0.5 mrad.

The thruster controller takes both position and rate error signals using the estimates from the estimator. The control law is simply a switching line of the form $e = -(\theta + K\omega)$, where e is the total error, θ is the position error, ω is the rate error, and K is the rate-to-position gain. The thruster controller currently uses K = 3 for maximum damping and minimum thruster activity. Because of the uncertainty in environment disturbance near Saturn and Titan, the controller has to be designed with robustness against plant uncertainties, such as variations in mass, inertia and minimum thruster impulse. The controller is designed to attenuate high frequency boom modes on one hand, and to be able to suppress the low frequency sloshing modes on the other.

The controller has a rate limiter used to damp the rate of the overall system. Rate saturation limits and their relative deadband can be implemented as a "position error limit" tied to the current deadband size and the maximum allowable spacecraft rate of 0.75 deg/sec.

In normal operations, eight thrusters are available for spacecraft 3-axis stabilization and turn maneuvers. The controller makes use of thruster firing logic to distribute the control torque in 3 axis into commands for the 8 thrusters for them to fire for certain time durations. There are two sets of thrusters: Y-facing and Z-facing. Y-facing thrusters control Z-axis motion and Z-facing thrusters control X & Y axes turns. Each thruster has a backup module to be used in case the primary one fails. The command variables to the attitude control thrusters are the thruster on, off and pulse duration.

Notch Filter

During the spacecraft close flyby at Titan where significant aerodynamic drag disturbance is expected, resonance of the magnetometer boom may be caused by thruster firings. To overcome such disturbance, the control thrusters may be firing at frequencies very near the magnetometer boom fundamental mode frequency. In such instance, the conventional bang-bang control can not cope with the dynamics excitation, and may become only marginally stable with lots of excessive thruster firing. To prevent such possible disturbance induced structure oscillation during Titan flyby, both position and rate error signals will be filtered before they get passed to the controller. A second-order notch filter is chosen which results in an acceptable amount of phase margin while tolerating up to 20 % uncertainty in the magnetometer boom frequency knowledge. Implementing such filter in the controller removes the atmospheric disturbance induced structure oscillation problem with reasonable stability and sensitivity margins.

Spacecraft Limit Cycle Control

Thruster valve operation cycles and propellant are valuable consumable especially for long mission spacecraft such as Cassini. In the entire Cassini mission, the cruise phase consumes about 65 % of total thruster cycle counts in the presence of low and steady environmental disturbance torque (e.g. solar torque). It is therefore crucial to enable the controller to have some “optimal” thruster impulse control to minimize the thruster cycles. A limit cycle profile with the least possible number of deadband encounters, and therefore minimum thruster firings, can be characterized by a profile of repeated “super cycles”. The ideal scenario is to fire a single pulse with the optimal impulse to push the spacecraft attitude to the opposite side of the deadband, and the body rate subsequently attenuates to zero before actually reaching the opposite edge. Rate attenuation is caused by the usually uni-directional environmental disturbance

torque which will eventually push the spacecraft attitude back towards the same deadband edge for another optimal thruster firing. This one-sided limit cycling with the longest possible time periods between deadband encounters is the most desirable situation during cruise to conserve thruster firing cycles.

Two limit cycle control features are added to the controller for reducing thruster cycles: the pulse width adjuster and the hysteresis or "walking" deadband. Both are effective only when the spacecraft is quite quiescent and cruising with very low rates below 50 μrad/sec. Such low-rate control schemes will be totally bypassed if regular thruster control activities are needed, such as turn maneuvers or during Titan flyby when large aerodynamic drag has to be overcome. The switching between regular thruster controls (nominally at high rate) and low rate limit cycle controls is autonomous within the controller based on a specified rate threshold value and other criteria.

One approach uses an adaptive pulse width adjuster to tune the thruster on-time based on the current and previous limit cycle peak magnitudes and uses the previous thruster on-time to determine the desired on-time for the next thruster pulse. Fig. 5 shows the limit cycle profile where d designates the peak to peak deadband size. Based on the measured limit cycle peaks L_1 and L2, one can compute the correction factor f for the next thruster on-time to achieve a desired next limit cycle peak L3. For a deadband incoming rate of Ω_1 and departure rate of Ω_2, we have $\Delta\Omega = \Omega_1 + \Omega_2 = \sqrt{2a}\, L_1 + \sqrt{2a}\, L2$ where "$\Delta\Omega$ " is the last rate change that cancels the incoming rate Ω_1 and sent the error position to achieve L2 limit cycle with the departure rate Ω_2. "a" is the external disturbance induced acceleration which is practically constant for short duration. Therefore, the peaks L_1 and L2 of the two adjacent limit cycles and the next desired limit cycle L3 can form the ratio of next thruster on-time correction factor "f', i.e. $\Delta\Omega' = \Omega_2 + \Omega_3 = \sqrt{2a}\, L2 + \sqrt{2a}\, L3 = \Delta\Omega * f$. The correction factor f is simply the ratio: $(\sqrt{L2} + \sqrt{L3}) / (\sqrt{L_1} + \sqrt{L2})$. The thruster on-time to change rate from Ω_2 to Ω_3 to achieve a next limit cycle peak of L3 will be the previous thruster on-time to change rate from Ω_1 to Ω_2 multiplied by the correction factor. After a few training cycles under nominal transient conditions, the pulse width adjuster can converge to what the formula predicts. Since this pulse width adjuster is purely based on position errors, the problems of noisy rate estimates and the need to estimate external disturbance and the associated uncertainty can be totally bypassed, Typical simulated times between consecutive one-sided deadband crossing is on the order of 10-30 min depending on the disturbance level.

The Cassini thrusters have a minimum on-time requirement of about 8.2 msec corresponding to 13 mNs at 400 psi which is the "floor" on the thruster adjuster (test data showed on-time as low as 5 msec). However, the small disturbance that requires below thruster minimum on-time is probably too small to matter any way. Cross coupling rate changes from other axes are also quite small to cause performance degradation of any significance.

A more realistic "threat" to the pulse adjuster performance is the randomness of thruster impulse which has variations from pulse to pulse. Such randomness can possibly prolong the two-sided limit-cycle transients with extra thruster firings before settling down to the desired limit cycle behavior. A possible solution (not implemented on Cassini) is to autonomously reduce the value of the pulse correction factor once two-sided limit cycle occurs. If two-sided limit cycling does occur too frequently in flight, it may be necessary to do in-flight tuning of the correction factor in the pulse adjuster.

A walking deadband is added to the controller to avoid the undesired phenomenon of "double pulsing". The need arises during most of the cruise phase when the external disturbance is so low that the resulting limit cycle rate is smaller than the rate noise, and additional thruster firing can be easily triggered by the rate noise. The walking deadband is activated only during cruise to save thruster pulsing cycles whenever deadband crossing occurs. A maximum of five consecutive walking steps are allowed. The deadband is reset to the initial size whenever the position error decreases to within 80% of the original deadband. The walking deadband implementation is very effective in preventing double pulsing, provided that the size of the walking step is set properly. In principle, the step size should be wider than the product of the expected maximum limit cycle rate and the time interval between successive control error evaluations. This way, when the control law is next evaluated subsequent to a deadband crossing, the error should stay within the expanded deadband.

The controller will raise a warning flag for imminent thruster firing two sec prior to any thruster firing so that science instruments can close covers for protection. This way, maximum time for science observation can be achieved without the need of building thruster firing protection time line in the command sequence. This will also reduce mission operation costs by eliminating thruster firing protection constraints in ground sequencing and planning,

Thruster Control Performance

The simulated thruster control performance has been shown to meet all the requirements for turning, detumbling, sun search and probe tracking. For sun search, the controller can follow the spiral sun search profile to better than 1 mrad accuracy at all times, and full sky sun search can be accomplished in less than 35 min. Fig 6 shows the spacecraft response after the Titan probe ejection. The initial spacecraft response to the force and torque impulse due to probe separation is 1,1 deg/sec rate in rotation and 0.4 m/see velocity in translation motion. The simulated spacecraft rate is clearly shown to have damped to less than 0.1 mrad/sec in less than 3 minutes. Spacecraft oscillations due to its response to propellant slosh is also quite apparent in the simulated response. Although attitude control has been temporarily disabled for a few seconds, attitude is continuously propagated by the attitude estimator based on the gyro data. This propagated attitude knowledge permits the spacecraft to quickly resume control and stabilization once the rate detumble maneuver is complete.

5.2 Precision Pointing Control

Precision pointing of the Cassini instruments is controlled by using the reaction wheels, Precision control is required for events such as Earth point for radar (Ka band) downlink and remote science observations and imaging. A typical precision pointing maneuver is a spacecraft slew start and stop followed by instrument staring for a certain exposure time. If a number of these slews are stacked together, they are called mosaics or strips. In most cases, the spacecraft will conduct a series of slow rotations to allow the camera or instrument boresight to cover the entire target or to follow target motions.

The reaction wheel controller design consists of a 3-axis proportional-integral-differential controller with 0.03 Hz bandwidth and 8 Hz sampling rate. The control law computes accelerations that will drive the attitude and rate estimates to the commanded values. Such computed acceleration is added to the feedforward acceleration commands from the attitude commander, and the result is scaled by the spacecraft inertia tensor to compute the desired reaction wheel torques. Integral control is set to zero at launch because the primary disturbance source that required the integral control is the reaction wheel friction,

which is already estimated and compensated within the control loop. Other external disturbances acting on the spacecraft such as solar wind or Titan atmospheric drag at high altitude that require the integral term are quite small and are well within the pointing error tolerance. Nevertheless, a non-zero integral control gain can be set in flight if it is determined that external disturbance torque exceeds current prediction.

The controller includes a rate and an acceleration limiter. The rate limiter limits the feedback rate with value set at around 20 μrad/sec. The acceleration limiter limits the feedback torque requested in each spacecraft axis as a result of existing rate errors. This limiter does not limit the magnitude of the feedforward acceleration and assumes it has been properly generated by the commander.

The controller performance is easily affected by the presence of large rate noise and has hence included a fourth-order low-pass rate filter used to filter the rate estimates. The filter coefficients are calculated by assuming that the poles of the filter are complex conjugates and can be described as a function of their damping factor and natural frequency. These damping and frequency values are selected by examining their effect on gain and phase margins. In particular, gains and filter coefficients are selected to provide adequate gain margin for the magnetometer boom resonance at 0.65 Hz, phase margin at possible worst case RPWS boom resonance up to 0.2 Hz, and on the proportional-differential controller phase margin. The design goal or rule-of-thumb is a phase margin of about 20 deg at 0.2 Hz and a gain margin of about 40 dB at 0,65 Hz.

Table 1 provides a summary of the control stability margin when star and gyro data are available for use. It assumes that the digital controller has a full 125 msec worst case software delay between commanded and applied torque, and propellant slosh at 30% fill-fraction. It is seen that the rigid body proportional-differential controller has higher margins than a standard control design goal of 6 dB gain and 30" phase margins. The flexible body margin also appears reasonable in the RPWS and magnetometer boom columns.

Table 1 Precision Pointing Control Stability MarSins

space-craft axis	Rigid Body Gain Margin	Rigid Body Phase Margin	RPWS Phase Margin (Nominal, Worst Case)	Mag Boom Gain Margin (Nominal,, Worst Case)
x	12.9 dB	41.9°	> 4 0 °, > 2 0 "	22dB, 10 dB
Y	12.3 dB	42.3"	>40°, >20°	58 dB, 46 dB
z	14.3 dB	40.1°	>40°, >20"	28 dB, 16 dB

The worst case scenarios in the last two columns of Table 1 reflect the frequencies of the flexible booms at their worst values within the possible range. For the magnetometer boom gain margins, the worst case value represents a degradation of the margin if the magnetometer boom frequency varies up to 15 %, but not below 0.65 Hz. For the RPWS antenna boom, the worst case value represents the margin if the RPWS booms are at a worst case frequency as high as 0.2 Hz.

Reaction Wheel Controller Design Constraints

Many of the design constraints, such as sensor noise, spacecraft structural flexibility, propellant slosh, and external disturbances, are factors affecting the choice of control loop bandwidth. There are trade-offs for accommodating these constraints, each affecting the other. In general, sensor noise and boom flexibility tend to drive down the controller bandwidth. Instrument settling time and disturbance

rejection needs against propellant slosh and instrument induced disturbance tend to push up the bandwidth. Given the noise and uncertainties such as sensor noise parameters, disturbance torque characteristics, flexible modes, etc. and the constraints based on allowable actuator torque and stability margins, one can use a constrained optimization program to find the particular controller required to optimize performance of the described system while conforming to the constraints. The final controller design with selected bandwidth and filter parameters has not only accommodated all the existing constraints, but also met pointing performance requirements.

Sensor noise with significant frequency content within the control bandwidth looks like valid commands to the controller. The controller then torques the spacecraft attitude to follow these erroneous "commands" which could result in undesired spacecraft motion. Such effect accounts for the largest component of spacecraft position stability performance in the absence of external disturbance torques. This effect can be minimized by lowering the controller's bandwidth such that high frequency sensor noise is not acted upon by the controller, and hence reducing the amount of undesired spacecraft motion.

Transient behavior due to slosh and structural excitation during the acceleration or deceleration phases of spacecraft slews causes undesirable spacecraft motion. The low-g propellant slosh appendage modes within the bandwidth of the control loop can cause transient position errors to occur at the beginning and ending of slews. This may result in an increase of settling time required before performance requirements are met. Loop shaping has been designed that increases the feedback gain around the propellant slosh frequencies. This effectively requires an increase of the control bandwidth to increase gain or reject disturbance at around slosh frequencies. To meet pointing stability, the control loop bandwidth is increased (results in faster time constants) and feedforward rate and acceleration commands are used for slews in order to reduce transient magnitudes.

The magnetometer boom appendage modes are far outside the bandwidth of the control loop, but have high structural gain of approximately 35 dB. Control-to-structure instability may occur due to high gain, gyro lag, and digital sampling rate induced phase lag. Gain stabilization of the boom modes in the controller design is accomplished by loop shaping with a low pass filter and a lower bandwidth to provide gain margin around magnetometer boom frequencies. On the other hand, the antenna boom for the radio and plasma wave science has fundamental appendage modes outside of the bandwidth of the control loop, but not by very much. As such they occur near the -180 degree phase transition area of the control loop and induce moderate structural gain of approximate y 15 dB. Control-to-structure interaction instability is not a problem as long as the modes occur before the -180 degree phase crossing. Again loop shaping is done to make sure sufficient phase margin exists around the RPWS frequencies, given the gyro lag, digital sampling rate induced phase lag, and the roll-off filter used for gain stabilization of the magnetometer boom.

Pointing Stability Performance

The control performance discussed here is limited to the pointing stability, which is defined to be the amount of position excursion over a given instrument exposure time period while the spacecraft is under reaction wheel control on gyros, and the Star ID is in its track mode. Fig 7 shows the simulations of spacecraft pointing stability about the worst axis (X), which has the largest attitude determination error because it is along the star track boresight or "twist" direction. This stability is defined by the angular position error (2 σ) relative to the target position expressed in the root-mean-square (RMS) sense. This means that for a given instrument time exposure (in see), stability is expressed in twice the standard

deviation of the pointing vector position relative to its mean. The time exposure or window size in Fig. 7 ranges from 0.1 sec to 1000 sec. Stability is computed after a 6 mrad spacecraft slew and allowing for both 20 sec and 5 min of settling time. For example, for a one-see exposure window, pointing stability is below 1.5 mrad (2σ) with no disturbance from instrument's articulating elements and 2.5 mrad (2σ) with instrument disturbance. Pointing stability performance is shown relative to the requirements of various instruments (image science subsystem, infrared spectrometer, etc). It is clear that stability requirements can be well met with margin of over 35 % in all cases.

5.3 Trajectory Correction Maneuver Control

The Cassini interplanetary mission requires both large and small trajectory correction maneuvers for navigation purposes. Almost all of the required velocity change or delta-V for trajectory correction is delivered by the 440 N bipropellant thrust from the main engine. Each main engine (redundant) is mounted in a gimbal system, allowing 2-axis articulation for thrust vector control during burns. Other smaller delta-vs are performed by the four thrusters along the $-Z$ direction. Attitude stabilization during such burns is. accomplished by "off-pulsing" of the firing thrusters. Bums are terminated based on the amount of delta-V accumulation. In the case of main engine burns, the accelerometer measures the delta-V accumulation. Since delta-V information is crucial for main engine burn during the Saturn orbit insertion, its estimate using main engine force impulse will be computed as a backup in the event accelerometer fails to provide measurements. In the case of delta-V burns using thrusters, the accumulation is computed from estimated thruster impulse. In both cases, the body-fixed delta-V magnitude is used by the attitude controller for burn termination.

Thruster Vector Control

The thrust vector control algorithm resides in the attitude controller. It articulates the main engine control axes perpendicular to the thrust vector. The third axis or the roll about the thrust vector is controlled using the reaction control thrusters. To start a burn, a command will point the thrust vector along the expected spacecraft center-of-mass. Attitude error is computed and then decomposed into orthogonal small-angle errors and is subsequently transformed to a coordinate system which has its third axis along the centerline of the initial main engine articulation. The components of these position and rate errors drive the two single-axis thrust vector controllers which outputs acceleration requests. These requests will be transformed into engine rotation commands, and then into extension commands for the engine gimbal actuators. The third axis position and rate errors also drive the roll control logic, which is a simple bang-bang controller with low rate-to-position gain. A wide deadband is used primarily to prevent thruster response to transient disturbances coupling from the thrust vector control axes.

The performance of the main engine burn depends on the ability of attitude control to keep the main engine thrust vector aligned with the desired delta-V direction. In order to minimize the maneuver errors and to keep spacecraft rates to an acceptable level during the transient after a burn ignition, it is desirable to push up the controller bandwidth. This way, the fundamental high-g slosh modes containing most of the slosh energy can also be within the thrust vector control bandwidth. However, the bandwidth is limited from above by the presence of the lightly-damped magnetometer boom fundamental bending mode. Although such zero-pole type appendage mode would provide stable interaction with a high bandwidth proportional-differential controller, the phase margin starts to degrade rapidly around 1 Hz. The phase lag is further worsened by the needed accommodation of a possible full interval of time sampling delay (125

msec). The final design is to gain-stabilize the magnetometer boom mode, with a thrust vector control bandwidth of 0.2 Hz, while slosh modes and RPWS modes are both phase stabilized.

Current controller for the spacecraft rigid body has a gain margin of 12 dB and phase margin of 30 degrees. With the thrust vector control bandwidth at much below the magnetometer boom fundamental mode, there is an adequate margin of 13 dB in the boom structural modes for stable interaction with the controller. Because of the expected high darnping in the slosh mode [5], the current thrust vector control design also has a factor of 30 margin in the combination of slosh damping and frequency uncertainty before getting into instability problem.

Thrust Vector Control Performance

During a main engine burn, the maximum rate experienced by the spacecraft is estimated to be 0.5 deg/s, and the axial acceleration to be 0.03 g. Fig. 8 (a) shows the spacecraft rate startup transient (in X axis) which peaks out at 0.5 deg/sec. The plot shows large disturbance of sloshing bipropellant in response to the translational acceleration from the main *engine* with superimposed magnetometer motion. During this burn, the engine deflection angle referenced to the pre-aim orientation can be as much as 3 deg from initial orientation with overshoot up to 2 deg. There are two error sources contributing to maneuver delta-V pointing error. The first contribution, referred to as proportional pointing error, is the steady-state misalignment of the thrust vector from the delta-V target. Its allocated requirement from the maneuver error budget is less than 4 mrad. Such error budget also contains other entries such as structural misalignments and attitude determination errors. The second contribution, referred to as fixed pointing error, is the lateral delta-V component which results from the transient response due to the pre-aim error. It is required to be less than 100 mm/sec for the uncalibrated case. The two errors are assumed to be independent, and their root-sum-squared value forms the total delta-V pointing error between the actual delta-V vector and the delta-V target vector. Fig. 8 (b) shows the delta-V pointing error as a function of maneuver termination time. The upper bound is the pointing error requirement. From the plot, it is clear that a bum of at least a minute is required in order to average the data over several cycles of the propellant slosh disturbance. The gimbal angle is driven based on the "pre-aim" error, which is the angle between the initial engine thrust vector and the vector from the engine gimbal through the system center of mass. Due to mass property uncertainties and various misalignments, this "pre-aim" error can be as large as 1 deg for the first bum.

6. Conclusion

A control design concept to achieve the many capabilities required for Cassini planetary missions to Saturn and Titan has been described. Attitude control has been designed to accommodate many challenges and constraints imposed by the mission, such as high percentage of liquid propellant (60 % at launch), lowly damped flexible appendages, and the need for minimizing thruster firing cycles. Selected computer simulation results have been given to demonstrate the design performance and capability. It has been shown that the Cassini attitude control design contains extensive autonomous capabilities, such as autonomous attitude determination and initialization, on-board gyro and accelerometer bias calibration, on-board adaptive pulse width adjuster for reducing thruster cycle counts, and the ability to detect and avoid constraints onboard (not described in detail in this paper). This represents a significant step towards the design and development of more autonomous capabilities in attitude control on future planetary spacecraft.

Acknowledgment

The authors appreciate the effort in the design and development of control algorithms by J. Alexander, R. Chiang, P. Enright, G. Macala, M San Martin, and G. Singh of the Cassini Control Analysis team. The research described in this paper was carried out by the Jet Propulsion Laboratory, California Institute of Technology, under contract with the National Aeronautics and Space Administration.

Reference:

[1] "Propellant Slosh Models for the Cassini Spacecraft" P. Enright and E. Wong, AIAA/AAS Conference, Scottdale, Arizona, Aug 1, 1994

[2] "Cassini Attitude Commander Algorithm" Gurkipal Singh, Jet Propulsion Laboratory Internal Memorandum, IOM 3456-94-020, Sep 12, 1994

[3] "The Cassini Spacecraft: Object Oriented Flight Control Software" J. Hackney, D. Bernard, R. Rasmussen, AIAA-AAS conference, 1993, paper No. 93-033, 1993

[4] "Inertial Attitude Determination for a Dual-Spin Planetary Spacecraft" E. Wong and W. Breckenridge, Journal of Guidance, Control, and Dynamics, Vol. 6, No 6, Nov. 1983

[5] "Cassini Propulsion Module Subsystem Slosh Models" James Tegart, CPMS-SM-001, Aug 1993, prepared for Jet Propulsion Laboratory by Martin Marietta Technologies, Inc.

[6] "Cassini Attitude Estimator Algorithm" Miguel San Martin, Jet Propulsion Laboratory Internal Memorandum, IOM 3456-94-024, Ott 12, 1994

[7] "Cassini Attitude Control by Reaction Wheels" Glenn Macala, Jet Propulsion Laboratory Internal Memorandum, EM 345-006, Nov. 15, 1994

[8] "Cassini RCS Attitude Control Algorithm" Richard Chiang, Jet Propulsion Laboratory Internal Memorandum, EM 345-005, Nov. 4, 1994

[9] "Cassini RCS RCS Delta-V Algorithm" Paul Enright, Jet Propulsion Laboratory Internal Memorandum, IOM 3456-94-016, Aug 29, 1994

[10] "Cassini Inertial Vector Propagation Algorithm" Gurkipal Singh, J-et Propulsion Laboratory Internal Memorandum, IOM 3456-95-001, Jan. 6, 1995

[11] " Star Identification Design Review" Jim Alexander, Jet Propulsion Laboratory Internal Memorandum, April 6, 1995

[12] "Behavioral Model Pointing on Cassini Using Target Vectors" R. Rasmussen, G. Singh, D. Rathbun, G. Macala. AAS 95-006, Feb. 1995.

[13] "Thrust Vector Control Algorithm Design for the Cassini Spacecraft" P. Enright, AIAA/AHS/ASEE Aerospace Design Conference, Irvine, CA, Feb. 16, 1993

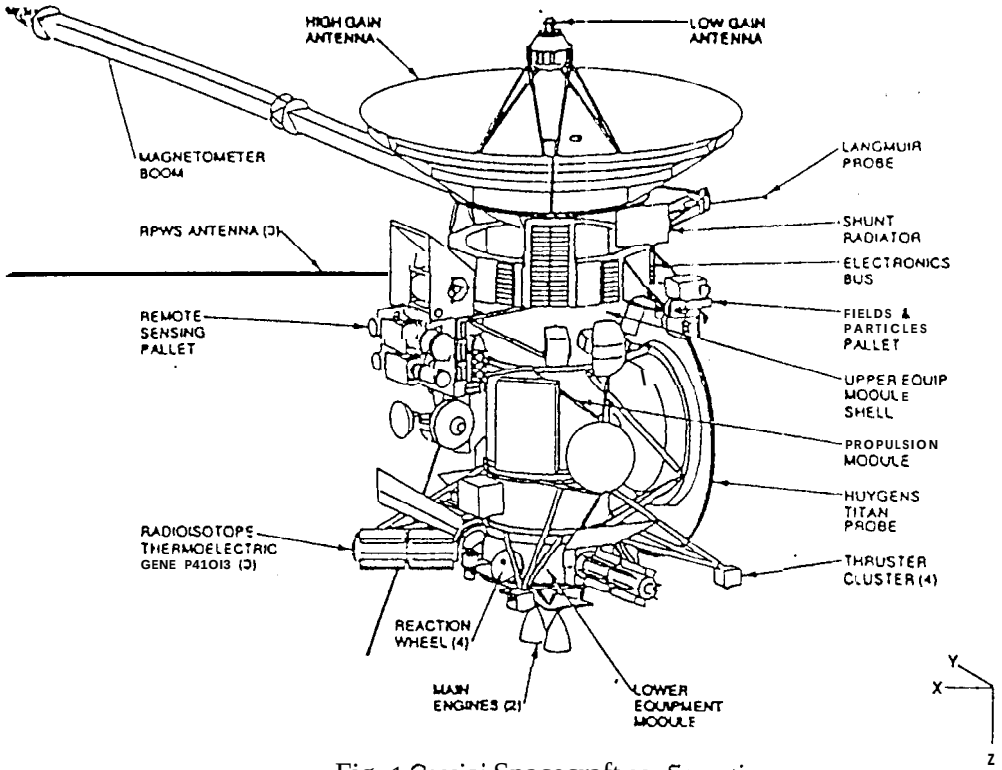

Fig, 1 Cassini Spacecraft configuration

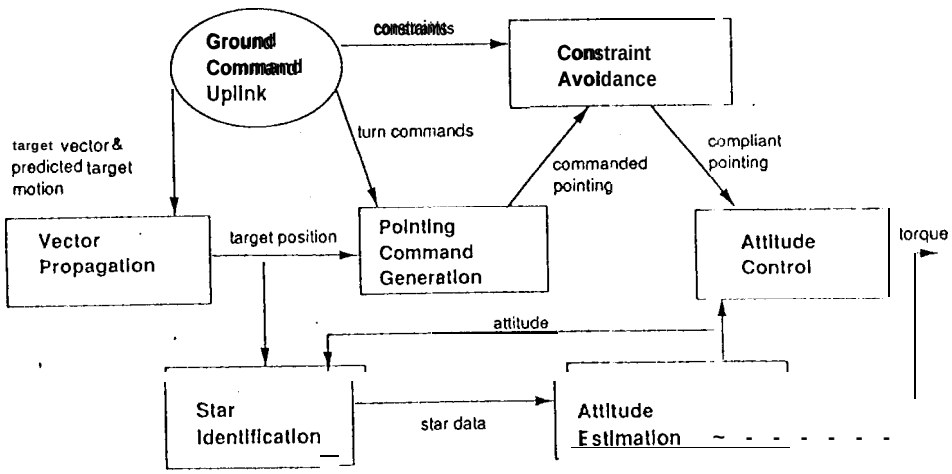

Fig. 2 Attitude Control Functional Block Diagram

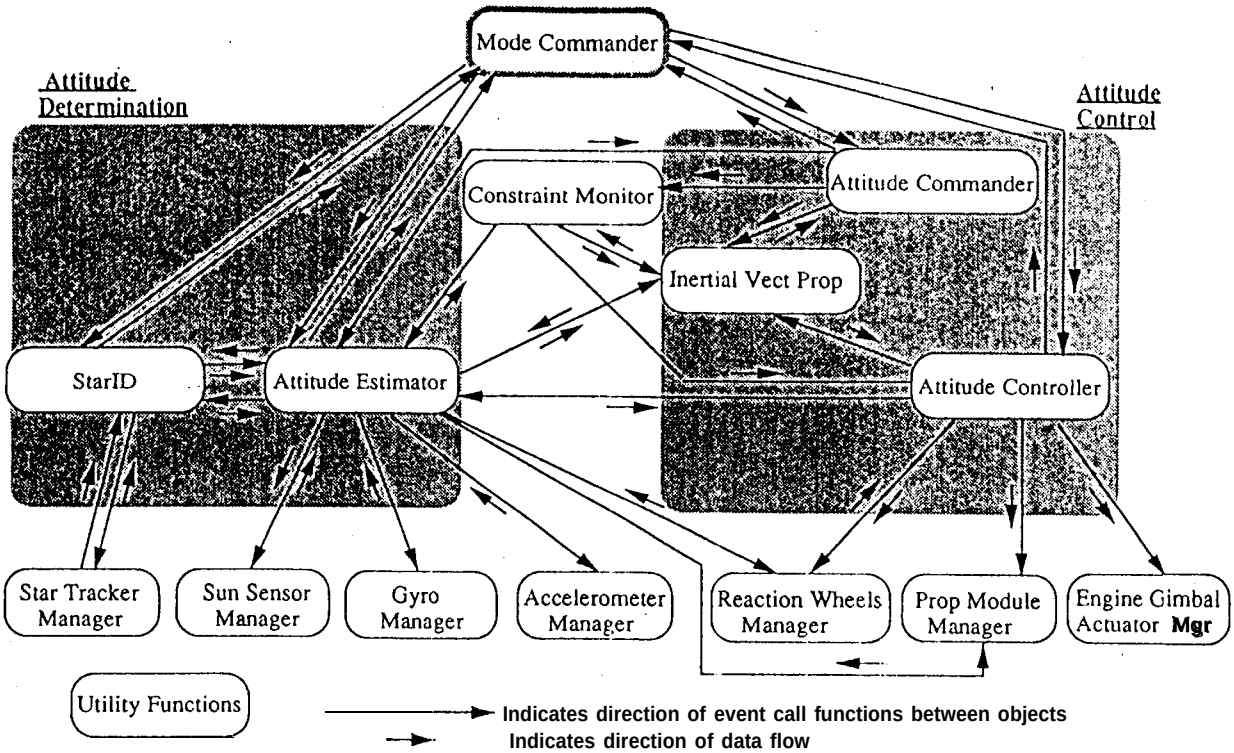

Fig. 3 Control architecture for Cassini

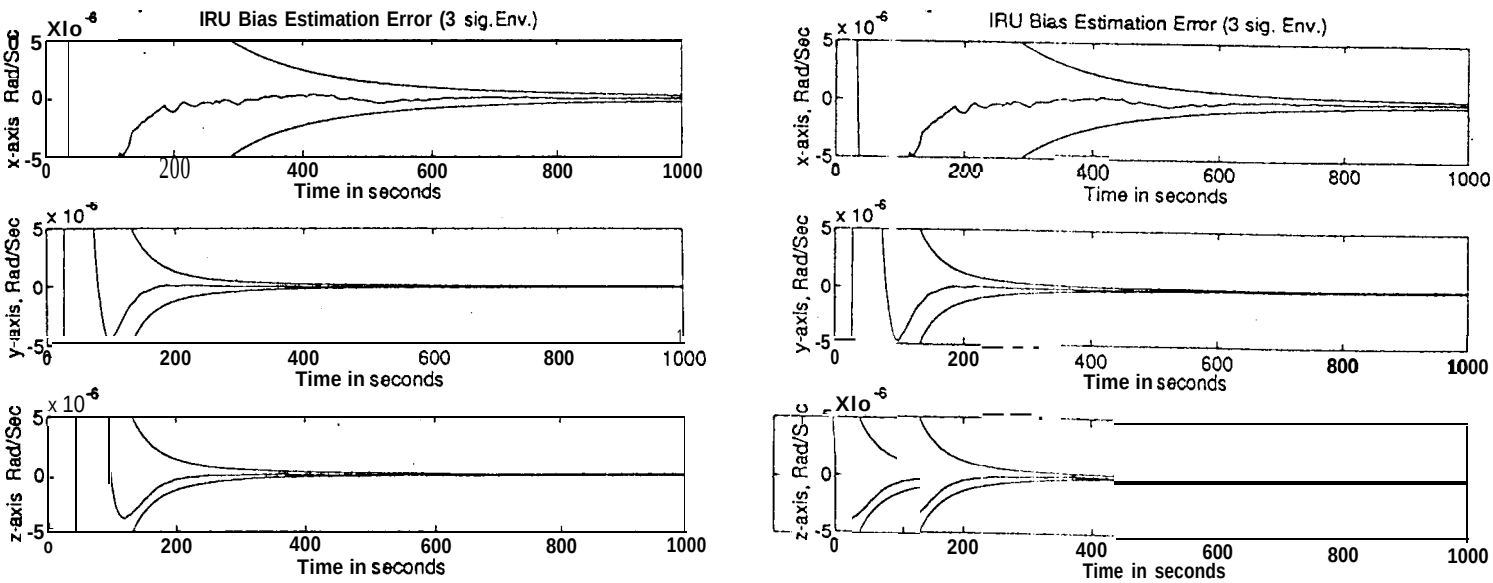

Fig. 4 Attitude Estimator Performance

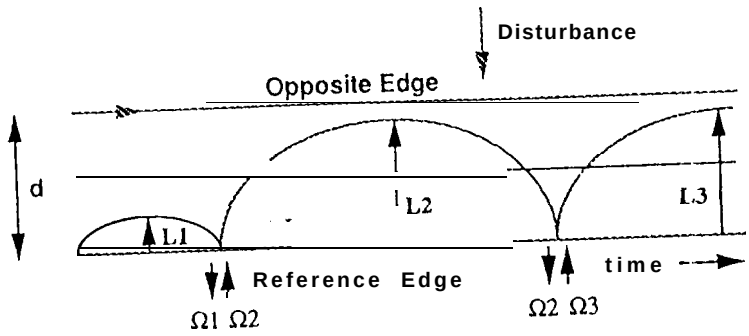

L1, L2, L3: Limit Cycle Peaks

Fig. 5 Adaptive Pulse Width for Control by Thrusters

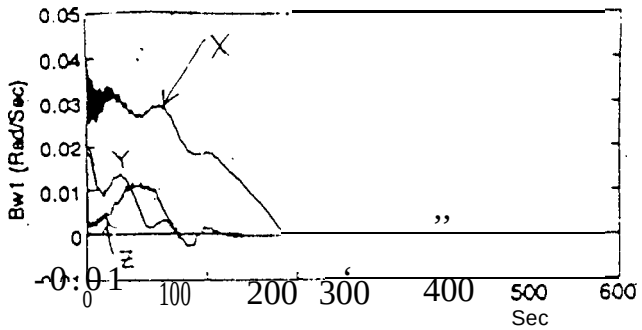

Fig. 6 Simulated Spacecraft Response after Probe Release

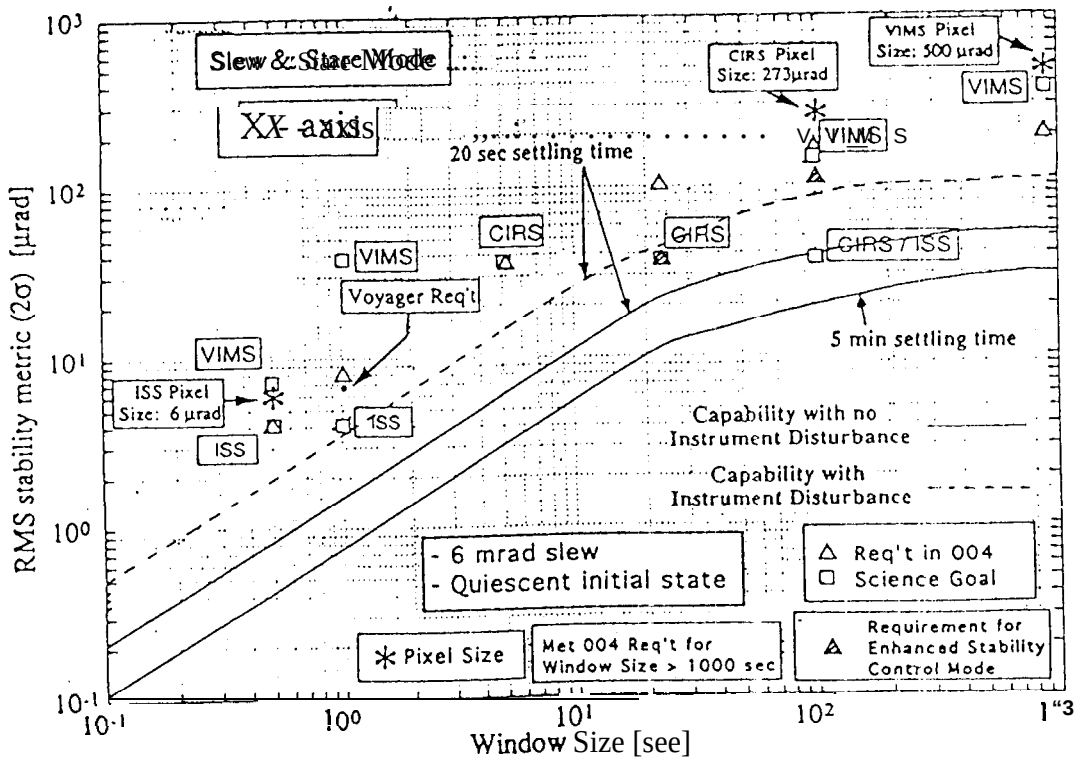

Fig, 7 Remote Science Pointing Stability Performance

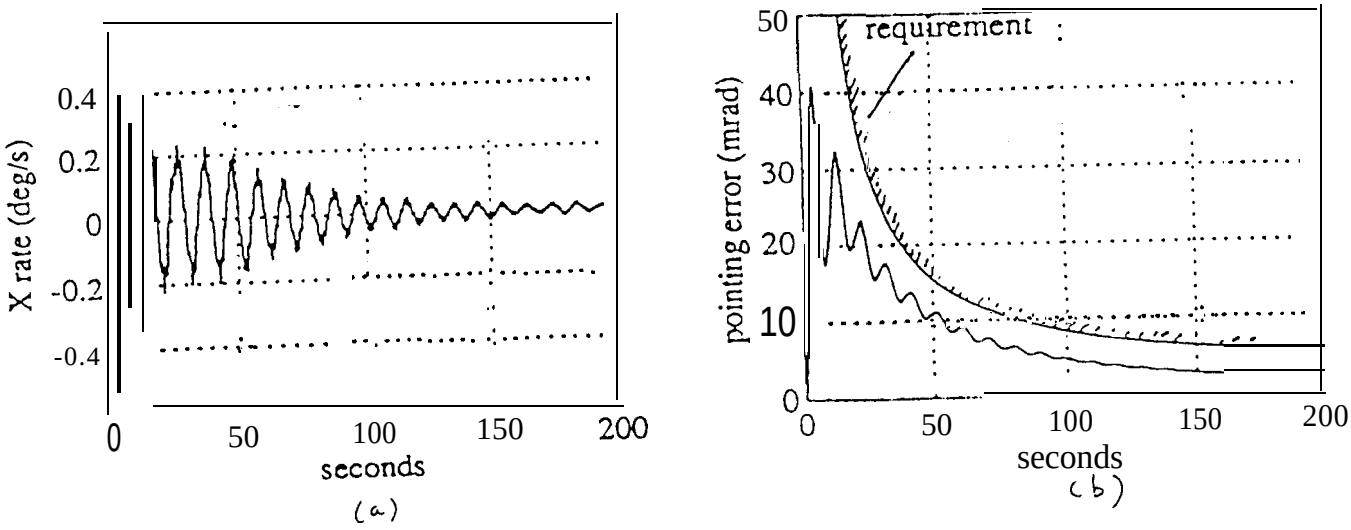

Fig, 8 Thrust Vector Control Performance